



Published in final edited form as:

Mol Imaging Biol. 2007 ; 9(3): 126–134. doi:10.1007/s11307-007-0079-2.

***In Vivo* Bioluminescence Tumor Imaging of RGD Peptide-modified Adenoviral Vector Encoding Firefly Luciferase Reporter Gene**

Gang Niu^{1,2}, Zhengming Xiong², Zhen Cheng², Weibo Cai², Sanjiv S. Gambhir², Lei Xing¹, and Xiaoyuan Chen²

¹Department of Radiation Oncology, Stanford University School of Medicine, Stanford, CA, USA

²Molecular Imaging Program at Stanford (MIPS), Department of Radiology and Bio-X Program, Stanford University School of Medicine, 1201 Welch Road, P095, Stanford, CA 94305-5484, USA

Abstract

Purpose—The goal of this study is to demonstrate the feasibility of chemically modified human adenovirus (Ad) vectors for tumor retargeting.

Procedures—E1- and E3-deleted Ad vectors carrying firefly luciferase reporter gene under cytomegalovirus promoter (AdLuc) was surface-modified with cyclic arginine–glycine–aspartic acid (RGD) peptides through a bifunctional poly(ethyleneglycol) linker (RGD-PEG-AdLuc) for integrin $\alpha_v\beta_3$ specific delivery. The Cocksackie and adenovirus viral receptor (CAR) and integrin $\alpha_v\beta_3$ expression in various tumor cell lines was determined by reverse transcriptase PCR and fluorescence-activated cell sorting. Bioluminescence imaging was performed *in vitro* and *in vivo* to evaluate RGD-modified AdLuc infectivity.

Results—RGD-PEG-AdLuc abrogated the native CAR tropism and exhibited significantly enhanced transduction efficiency of integrin-positive tumors than AdLuc through intravenous administration.

Conclusion—This approach provides a robust platform for site-specific gene delivery and noninvasive monitoring of the transgene delivery efficacy and homing.

Keywords

Adenovirus; Firefly luciferase; Reporter gene; Integrin $\alpha_v\beta_3$; RGD; Bioluminescence imaging

Introduction

The human adenovirus (Ad) was widely used as a vector for delivery of foreign genes to mammalian cells because of its relatively high efficacy in accomplishing gene transfer *in vivo* [1]. Recently, it was suggested that the binding of adenovirus to its primary receptor, Cocksackie and adenovirus viral receptor (CAR), may be an important rate-limiting step for

gene transfer [2]. Although CAR is expressed ubiquitously on most normal epithelial cells, CAR expression in tumors may be highly variable, resulting in insufficient transduction of tumor cells [3]. Biodistribution studies of systemically administered adenovirus revealed that in rodents and nonhuman primates, adenovirus preferentially accumulates in the liver and to a less extent in the spleen [4, 5]. Hepatic uptake of adenovirus presumably takes place mainly via CAR on the hepatocyte, although detailed information about the mechanisms of entry to other cell types remains to be elucidated. To compensate for such sequestration, significant escalation in the doses of administered vector is needed to achieve efficient gene transfer to those cells with no or insufficient CAR expression. This, in turn, increases the risk of inducing both direct toxicity and immune response against the vector, thus further compromising the overall efficacy of the therapy [6]. The toxicity due to vector dissemination to nontarget cells occurs even when Ad vectors are locally administered to the tissue of interest [7]. Vector targeting to a specific tissue or cell type would enhance gene therapy efficacy and permit the delivery of lower doses, which would result in reduced toxicity [8–10].

Cell-specific gene delivery via Ad vectors was achieved by a variety of approaches, including genetic modification of Ad capsid [8, 11–13], modification by the use of adaptor molecules [14–17], and chemical modification by polymers with ligand [18]. Genetically, two approaches were used to modify the fiber proteins: one is to add foreign peptides to the HI loop or C terminus of the fiber knob, the other is to substitute fibers derived from other Ad stereotypes, which bind to receptor molecules other than CAR. In this approach, one of the drawbacks encountered was that genetic modification of the virion capsid and/or fiber knob did not eliminate the endogenous tropism of the virus to the desired extent. Retargeting of Ad vectors can also be achieved through the use of bispecific or bifunctional adaptor molecules composed of an antifiber antibody fragment and a cell-binding component. Combination of the adaptor molecule and genetically modified capsids of the Ad vector was also reported. Chemical modification is a nongenetic strategy to modify the surface of the virion by covalently attaching a polymer containing the targeting ligand to the surface of Ad.

Chemical modification of Ad vectors with poly(ethyleneglycol) (PEG; PEGylation), in which the activated PEG reacts preferentially with the ϵ -amino terminal of lysine residues on the capsid, including the hexon, fiber, and penton base, prolongs persistence in the blood and circumvents neutralization of the Ad vectors by antibodies [19–22]. Furthermore, PEGylated Ad vectors attenuate the ability of the vector to be taken up by antigen-presenting cells, thereby reducing inflammatory responses. Animals injected with PEGylated Ad vectors exhibited reduced levels of both cell-mediated and humoral immune responses, resulting in significant gene expression on readministration of unmodified Ad vectors in the lung [19, 21]. However, the PEGylation of Ad vectors leads to loss of infectivity due to steric hindrance by PEG chains. The extent of loss of infectivity and extension of blood retention half-time are dependent on the degree of PEG modification [23]. Ad vectors coated with polymers other than PEG were also developed [18, 24].

To overcome the decreased efficiency of infection of PEGylated Ad vectors, vectors containing functional molecules on the tip of PEG were developed [23, 25, 26]. Lanciotti *et al.* modified Ad vectors by using heterofunctional PEG and FGF2 [25]. The transduction of

FGF2-PEG-Ad is dependent on the FGF2 receptor, and is almost independent of CAR. In an intraperitoneal model of ovarian cancer, FGF2-PEG-Ad led to increased transgene expression in tumor tissue and reduced localization of the vectors to nontarget tissues compared with unmodified Ad vectors. Ogawara *et al.* reported PEGylated Ad vectors containing E-selectin specific antibody at the tip of PEG, which target activated endothelial cells [26]. They showed that the systemic administration of PEGylated Ad vectors with anti-E-selectin antibody selectively targeted inflamed skin and mediated local transgene expression in mice with a delayed-type hypersensitivity (DTH) inflammation.

Integrin $\alpha_v\beta_3$ is highly expressed on activated endothelial cells and tumor cells but is not present in resting endothelial cells and most normal organ systems, making the receptor a potential target for antiangiogenic strategy [27–29]. The inhibition of $\alpha_v\beta_3$ integrin activity was also associated with decreased tumor growth in both clinical trials and small animal studies [30–34]. During the last few years, we and others have developed a series of arginine–glycine–aspartic acid (RGD) peptide probes for multimodality imaging of tumor integrin expression, including positron emission tomography (PET) [35, 36], single-photon emission computed tomography [37], and near-infrared fluorescence [38]. In this study, we modified E1- and E3-deleted adenoviral vectors encoding firefly luciferase reporter gene (AdLuc) with a cyclic RGD peptide through a bifunctional PEG linker and evaluated the integrin-specific transduction of RGD-PEG-AdLuc *in vitro* and *in vivo* by means of noninvasive bioluminescence imaging.

Materials and Methods

Cell Culture and Adenovirus Production

Recombinant adenoviral vector AdLuc expressing the reporter gene firefly luciferase under the control of cytomegalovirus (CMV) promoter was constructed as previously described [39]. The vector was amplified in 293T cells and purified by double cesium chloride ultracentrifugation. The purified virus was extensively dialyzed against 3% sucrose/phosphate-buffered saline and stored in aliquots at -80°C . The number of viral particles was determined by measuring the optical density of virus at 260 nm (OD_{260}). Determination of virus particle titer was accomplished spectrometrically. The ratio between virus particle number (vp) and plaque forming units (pfu) was found to be 30:1. Both mPEG (MW = 2,000) and NHS-PEG-MAL (MW = 3,400) were obtained from Nektar Therapeutics (San Carlos, CA, USA)

Chemical Modification of Adenovirus Tropism

Cyclic pentameric RGD peptide c(RGDyK) was conjugated with *N*-succinimidyl-*S*-acetylthioacetate (SATA) through the ϵ -amino group on the RGD peptide lysine residue under slightly basic condition. PEGylated AdLuc particles with and without RGD were prepared and the degree of conjugation was measured following a previously described procedure [40].

Flow Cytometry and Reverse Transcriptase PCR

Of the three cell types used for *in vitro* transduction studies (U87MG, MDA-MB-435 and MCF-7), the expression levels of integrin $\alpha_v\beta_3$ were determined by flow cytometry. The primary antibody specific for human integrin $\alpha_v\beta_3$ is Abegrin™ (MedImmune, Gaithersburg, MD, USA) and the secondary antibody is fluorescein isothiocyanate-conjugated donkey anti-human IgG antibody (Jackson ImmunoResearch, West Grove, PA, USA). The same secondary antibodies alone served as the negative control for each cell line.

Total RNA was extracted from freshly isolated MCF-7, U87MG, and MDA-MB-435 cells using RNeasy Kit (Qiagen Inc., Valencia, CA, USA). Four micrograms of RNA from each cell was converted into cDNA with Superscript III reverse transcriptase (Invitrogen Corp., Carlsbad, CA, USA). Then 200 ng cDNA was used for PCR amplification using CAR-specific primers: sense, 5'-GAGTAGTGGATTTCGCCAGAAGTT-3'; antisense, 5'-AAGCGTAAATTTGCATGGCAG-3'. The product length was 101 bp. Ten microliters of the product was used for 2% agarose gel electrophoresis.

In Vitro Transduction and Measurement of Firefly Luciferase Activity

To evaluate the *in vitro* transduction efficiency of AdLuc, PEG-AdLuc, and RGD-PEG-AdLuc vectors, cells (MCF-7, U87MG, and MDA-MB-435) were seeded in 12-well plates (5×10^5 cells per well) and infected 48 hours later with 10^3 virus particles per cell in triplicates in culture medium with 2% fetal bovine serum and incubated for four hours at 37°C. The incubation medium was then replaced by normal medium and cells were further incubated for 24 h. The luciferase activity was measured with Xenogen In-Vivo Imaging System IVIS200 (Xenogen Corp., Alameda, CA, USA). A 150- μ g/ml luciferin was added to each well for five minutes of incubation. Then the plates were put into the chamber of CCD camera for one-minute exposure. Region of interest (ROI) was outlined on each well. Photon flux was quantified by the software provided by the manufacturer. The luciferase activity was expressed as photon flux per second per million cells. For RGD blocking, 20 μ g/ml of RGD peptide was added 30 minutes before adenovirus infection.

Animal Models

All experimental procedures involving animals were conducted in accordance with the institutional guidelines set forth by Stanford University School of Medicine. Immunodeficient female athymic nude mice were housed in specific pathogen-free facilities. The MDA-MB-435 breast cancer model was established by orthotopic injection of 5×10^6 cells into the left mammary fat pad. The U87MG glioblastoma model was obtained by injecting a mixture of 5×10^6 cells suspended in 50 μ l of medium and 50 μ l matrigel (BD Biosciences, San Jose, CA, USA) into the right front leg of nude mice. The mice were used for intratumor and intravenous viral administration when the tumor volume reached 500–700 mm³ (three to four weeks after inoculation).

In Vivo Transduction and Reporter Gene Analysis

For intratumor injection, AdLuc, PEG-AdLuc, or RGD-PEG-AdLuc at a dose of 2.5×10^9 vp/kg was applied intratumorally by multiple injections to MDA-MB-435 tumor-bearing

mice ($n = 3$ per group). For intravenous injection, 1.25×10^{12} vp/kg of AdLuc, PEG-AdLuc, or RGD-PEG-AdLuc was introduced via tail vein into each tumor-bearing mouse ($n = 3$ per group). Forty-eight hours later, the mice were subjected to optical imaging on the Xenogen IVIS200. Mice were anesthetized with 2% isoflurane and injected with α -luciferin (10 mg/kg intraperitoneal injection) approximately ten minutes before imaging. Images of the ventral and dorsal sides of the mice were taken. Light emitted from the tumors and liver was quantified using Living Image Software (Xenogen). Photon produced by luciferase was normalized as photons per second per centimeter squared per steradian ($\text{p s}^{-1} \text{cm}^{-2} \text{sr}^{-1}$). Twenty-four hours after imaging, the animals were killed. The liver, spleen, kidneys, lung, heart, and tumor tissues were harvested and homogenized in LAR-II reagent (Promega, Madison, WI, USA), then incubated for 20 minutes at room temperature. The luciferase activity was measured using a TD-20/20 Luminometer (Promega) after short vortex. Protein levels were determined by micro-BCA assay (Pierce, Rockford, IL, USA). The luciferase activity was normalized as relative light units (RLU) per milligram of protein.

Results

Chemical Modification of AdLuc Vectors

The schematic structure of RGD-PEG-AdLuc is shown in Fig. 1. The sulfhydryl addition agent SATA reacts with the lysine ϵ -amino group on the cyclic RGD peptide c(RGDyK) to form a stable amide bond. The product was confirmed by the disappearance of RGD peptide peak at 10.9 minutes and appearance of SATA conjugate peak at 12.1 minutes on the analytical high-performance liquid chromatography. Deacetylation of SATA with hydroxylamine gives quantitative yield of c(RGDy(ϵ -thioacetyl)K) ($t_{\text{Ret}} = 10.6$ minutes). The bifunctional NHS-PEG-MAL was first reacted with the AdLuc capsid protein amino groups. Without separating the unreacted PEG from the PEGylated Ad particles, the reaction mixture was added thiolated RGD peptide to form RGD-PEG-AdLuc. Excess amount of PEG and RGD peptide was removed by size-exclusion chromatography. RGD-PEG-AdLuc was recovered in the void volume of the PD-10 column. PEG-AdLuc conjugate was generated in a similar manner except that monofunctional PEG (mPEG-NHS) was used and no RGD peptide was coupled to the viral vectors. To identify the extent of viral surface modification by PEGylated RGD peptide and mPEG, we performed fluorescamine assay [41]. Fluorescamine reacts with the primary amino groups found in terminal amino acids and the ϵ -amine of lysine to form fluorescent pyrrolinone type moieties. Under standard conditions (10^5 PEG/viral particle), about 55–60% of the primary amino groups on the virion surface were substituted. Because the apparent molecular weight of an unmodified Ad particle is approximately 1.5×10^8 Da, with a diameter of 90–110 nm [42, 43], the PEG-RGD and PEG-modified AdLuc is estimated to have apparent molecular weight of 1.9×10^8 and 1.8×10^8 Da, respectively. The average particle size of PEG-AdLuc and RGD-PEG-AdLuc is thus estimated to be 10–15 nm bigger than that observed for the unmodified AdLuc.

In Vitro Infectivity of AdLuc, mPEG-AdLuc, and RGD-PEG-AdLuc

To investigate the infectivity of RGD-modified adenoviral vectors, U87MG, MDA-MB-435, and MCF-7 cells with different CAR and $\alpha_v\beta_3$ integrin expression levels as described in Fig.

2A, B were infected with AdLuc, PEG-AdLuc, and RGD-PEG-AdLuc, and the results were shown in Fig. 2C. For the unmodified AdLuc, the infectivity follows the order of U87MG > MCF-7 > MDA-MB-435. The infectivity of the AdLuc in three tumor cell lines is consistent with their CAR mRNA levels, suggesting CAR dependence of such transduction. The infectivity of mPEG-AdLuc is about two to three orders of magnitude lower than unmodified AdLuc in all three cell types examined, indicating that PEGylation shielded the interaction between the fiber knob and CAR. Compared with unmodified AdLuc, the infectivity of RGD-PEG-AdLuc vector on MDA-MB-435 cells was significantly increased ($P < 0.01$) and was efficiently blocked by free RGD. For U87MG and MCF-7 cells, the RGD-PEG-modified AdLuc also showed sharply enhanced transduction than PEG-AdLuc, although RGD peptide tagging did not fully restore the infectivity of unmodified AdLuc.

Intratumoral Administration of AdLuc, mPEG-AdLuc, and RGD-PEG-AdLuc

To observe the alteration of transduction after local administration of chemically modified AdLuc vectors, we performed noninvasive bioluminescence imaging scans (Fig. 3). As expected, PEG-AdLuc had minimal infectivity as quantified by ROI analysis of the light signal emitted from the orthotopic MDA-MB-435 tumor. It is also notable that the infectivity of RGD-PEG-AdLuc was about 1.8 times that of AdLuc, which was consistent with the *in vitro* assay. No significant difference in tumor infectivity was found for intravenously administered AdLuc and AdLuc-PEG, which is inconsistent with the *in vitro* infectivity assay. This indicated that most of AdLuc viral particles were intercepted by the liver after tail vein injection and only very small fraction may have reached tumors (Fig. 3)

Intravenous Administration of AdLuc, mPEG-AdLuc, and RGD-PEG-AdLuc

The ultimate goal of this study is to allow systemic administration of Ad vectors with a preferential tropism for target cells, which is otherwise not possible for unmodified Ad vectors. The promising *in vitro* and intratumor results prompted us to assess the *in vivo* kinetics, homing, and transgene expression of chemically modified Ad vectors after tail vein injection into xenografted mice. For this purpose, three groups of mice ($n = 3/\text{group}$) bearing both subcutaneous U87MG glioma (dorsal) and orthotopic MDA-MB-435 breast cancer (ventral) tumors were injected with AdLuc, mPEG-AdLuc, and RGD-PEG-AdLuc at the same dose of 1.25×10^{12} vp/kg (Fig. 4). Forty-eight hours later, mice were anesthetized and injected with β -luciferin approximately ten minutes before imaging. Light emitted from the tumors and the liver tissue was then quantified by ROI analysis. Twenty-four hours after noninvasive imaging when all the β -luciferin had cleared from the body the animals were killed and luciferase activity in the tumors and all major organs were analyzed by luminometer assay (Fig. 5).

As expected, the unmodified AdLuc had predominant liver (ventral imaging) and low tumor luciferase signal (dorsal imaging for U87MG and ventral imaging for MDA-MB-435 tumors). PEGylated AdLuc (mPEG-AdLuc), on the other hand, showed minimal transduction efficiency in all the organs as determined by both *in vivo* imaging and *ex vivo* tissue lysate luciferase assays, which further confirmed that the steric hindrance induced by PEG chain prevents the entry of the virion into cells. Transgene expression in the tumors and liver 48 hours after intravenous injection of RGD-PEG-AdLuc was measured by ROI

analysis of the luciferase signal using the Xenogen IVIS200 system. Fig. 5 shows that the transduction efficiency of the RGD-PEG-AdLuc was approximately 3-fold lower in the liver, 20-fold higher in U87MG tumor, and 6- to 7-fold higher in MDA-MB-435 tumor than the transduction efficiency of unmodified AdLuc. Fig. 5 also showed that RGD-PEG-AdLuc had slight but significant ($P < 0.01$) increase of spleen luciferase activity defined as RLU per milligram of protein.

Discussion

In our previous studies we have shown that firefly luciferase can be successfully used for real time imaging in living animals using a cooled CCD camera [44]. Such approach provides rapid, convenient, and inexpensive assays to monitor the location, magnitude, and duration of gene expression after somatic DNA transfer, all without the need to kill animals after each experimental procedure. The results obtained from *in vivo* images have good correlation with that from *ex vivo* luminometer assays. There is also a good linear relationship between the luciferase enzyme activity and the peak height of emitted light in a wide range of enzyme concentrations. The aim of this study was to explore the *in vivo* infectivity of RGD peptide-modified adenoviral vectors after intravenous administration into xenografted mice. We also investigated whether noninvasive bioluminescence imaging is a suitable method to assess the *in vivo* homing and transgene expression of the chemically modified adenovirus encoding firefly luciferase reporter gene.

PEGylation was proven as an effective method to prolong the retention time of adenovirus in blood, to protect the vector from host cellular and humoral immune response, and to relieve hepatic injury induced by the interaction between virus and host defense system [19–22]. These superiorities are attributed to the fact that PEGylation could effectively ablate the interaction of viral knob with its receptors (CAR and other receptors). Our *in vitro* transduction study in both CAR-positive and CAR-negative cells have shown that PEGylated adenoviral vector exhibits two to three orders of magnitude lower infectivity than the unmodified virus. Obviously, PEG molecules completely blocked the native tropism of adenoviral vector even at relatively low level of modification (55–60% surface modification in our case). Both noninvasive bioluminescence imaging and *ex vivo* tissue luciferase assay showed significantly reduced infectivity in the liver where CAR expression is abundant (Figs. 4 and 5). No significant difference in tumor infectivity was found for intravenously administered AdLuc and AdLuc-PEG, indicating minimal CAR expression in MDA-MB435 and U87MG tumors.

The integrin $\alpha_v\beta_3$ expression determined by flow cytometry followed the order of U87MG > MDA-MB-435 > MCF-7. The infectivity of RGD-PEG-AdLuc followed, however, the order of U87MG > MCF-7 > MDA-MB-435. MCF-7 cells with higher CAR and lower integrin expression showed higher infectivity than MDA-MB-435 cells, which suggests that RGD-PEG-AdLuc infected MCF-7 cells via dual recognition of CAR and integrin $\alpha_v\beta_3$ and that CAR-induced infectivity might be stronger than integrin. However, the higher infectivity of RGD-PEG-AdLuc than AdLuc in MDA-MB-435 cells demonstrated that RGD recognition by integrin $\alpha_v\beta_3$ played a more important role than CAR in this cell line because CAR expression in this cell line is extremely low [40]. This was further demonstrated by the fact

that the infectivity of RGD-PEG-AdLuc in MDA-MB-435 cells decreased significantly ($P < 0.01$) when blocked with free RGD, whereas the infectivity in MCF-7 cell was only slightly influenced ($P > 0.05$). It is also noticeable that in low integrin $\alpha_v\beta_3$ expressing MCF-7 cells, mPEGylation completely abrogated the transfection; however, RGD modification restored the infectivity of the adenovirus. One possibility is that although MCF-7 cells are $\alpha_v\beta_3$ -negative, they are α_v -positive. RGD-PEG-AdLuc may bind to α_v integrin and result in enhanced transfectivity. Another possibility is that mPEG-AdLuc is not necessarily the ideal negative control for RGD targeting. It is preferred to compare RGD-PEG-AdLuc with a scrambled RGD peptide conjugate. The size of the PEG is also different between mPEG-AdLuc (MW = 2,000 for mPEG) and RGD-PEG-AdLuc (MW = 3,400 for NHS-PEG-MAL). Whether such difference will have effect on the tropism of the chemically modified AdLuc is not known.

The general concept of the modification of Ad vectors with bifunctional PEG and homing ligands was reported earlier [23, 25, 26]; in this study, for the first time we showed that noninvasive bioluminescence imaging is able to quantify the gene expression of chemically modified adenoviral vectors carrying firefly luciferase reporter gene that lead to integrin-selective gene transfer into tumors. Although the *in vitro* infectivity of RGD-PEG-AdLuc did not fully restore the infectivity of AdLuc, it showed higher luciferase signal after local injection into MDA-MB-435 tumors. We have previously tested the integrin expression of tumor tissue vs. tumor cells based on sodium dodecyl sulfate polyacrylamide gel electrophoresis/autoradiography and found that as normalized to the same amount of protein, MDA-MB-435 tumor tissue lysate had four- to fivefold higher integrin than the tumor cells cultured *in vitro* [45]. This difference is most likely due to the fact that MDA-MB-435 cells grown *in vivo* tend to produce more integrin and that tumor vasculature in this tumor model express even higher amount of integrin.

Although intratumoral injection of RGD-PEG-AdLuc somewhat reflects the integrin specificity of the modified viral vectors, it does not tell whether the RGD-PEG-AdLuc is able to home to integrin-positive tumors and organs after systemic administration. We thus monitored the tumor targeting efficacy and whole body distribution of the three adenoviral vectors (AdLuc, mPEG-AdLuc, and RGD-PEG-AdLuc) after tail vein injection. As expected, there is minimal infectivity of PEG-AdLuc *in vivo*, which is also confirmed by *ex vivo* luciferase assay. It is worth mentioning that the enhancement of tumor infectivity of RGD-PEG-AdLuc compared to AdLuc after intravenous injection is significantly higher than that after intratumoral injection. Although not tested in this study, it was reported that PEGylated adenoviral vectors and other polymer-coated virus could increase blood circulation time and reduce innate immune response [46, 47]. We assume that RGD-PEG-AdLuc would have similar plasma half-life as mPEG-AdLuc, but substantially longer half-life than AdLuc. Significantly more amount of RGD-PEG-AdLuc is also expected to home into the integrin-positive tumor vasculature and tumor cells than mPEG-AdLuc and AdLuc that do not recognize $\alpha_v\beta_3$. Because intratumoral injection of the viral particles has already demonstrated more effective transgene delivery of RGD-PEG-AdLuc than AdLuc and mPEG-AdLuc, it is highly likely that the combined effect of prolonged plasma circulation

time, more effective tumor homing, and enhanced gene delivery is responsible for the overall excellent tumor infectivity of RGD-PEG-AdLuc.

It is not surprising that the RGD-PEG-AdLuc still showed some infectivity in the liver and spleen, although the extent of transgene expression in the liver is significantly lower. The mononuclear phagocytes of the reticuloendothelial system (part of the body's immune system, mostly concentrated in the liver, spleen, lymph nodes, and bone marrow) mediates nonspecific uptake of circulating viral particulates such as AdLuc, PEG-AdLuc, and RGD-PEG-AdLuc [48, 49]. Furthermore, the mouse liver with both CAR (high level) and integrin (low to medium level) would facilitate the infection of the incompletely modified RGD-PEG-AdLuc that homed to the liver. Further improvement to reduce the liver and spleen infectivity is thus needed to decrease the toxicity of the systemically administered tumor-targeted viruses.

Despite the success of this approach to retarget RGD-PEG-AdLuc to integrin-positive tumors, the construct will not be effective for integrin-negative tumors. Even for integrin-positive tumors the tumor infectivity is limited by the total number of receptors available for retargeting. The virus particle with over 10,000 free amine groups on the surface provides an excellent platform for coupling multiple ligands simultaneously to the surface of the same particle [25]. The total number of targets is thus substantially increased although the number of each receptor on the target cell is unaltered. This, if true, will further increase the efficiency and specificity of the chemically modified adenoviral vectors. The choice of firefly luciferase for *in vitro* and *in vivo* studies using a CCD camera is because the optical reporter gene imaging technique is convenient, fast, and relatively inexpensive [50, 51]. However, the attenuation, scatter, and resolution limitations of this technique limited its clinical use. PET reporter gene such as HSV1-tk or its mutants may be more advantageous for clinical translation [39, 52, 53].

In this study, E1- and E3-deleted Ad vectors carrying firefly luciferase reporter gene under CMV promoter (AdLuc) was surface-modified with cyclic RGD peptides through a bifunctional poly(ethyleneglycol) linker (RGD-PEG-AdLuc) for integrin $\alpha_v\beta_3$ specific delivery. We demonstrated that RGD peptide-modified adenoviral vectors through PEG linker on the fiber knobs allowed systemic administration for substantially increased tumor infectivity than unmodified AdLuc and PEGylated AdLuc based upon integrin recognition by means of noninvasive bioluminescence imaging. Adenoviral vectors with a preferential tropism for target cells will allow systemic administration for targeting both primary tumors and metastatic lesions, which is otherwise not possible for unmodified adenoviral vectors. As a nongenetic one-step process, this technology is simple, versatile, and yields vectors with an improved efficacy profile. This approach provides a new means for delivering therapeutic gene fused with reporter gene for site-specific gene delivery and noninvasive monitoring of the transgene delivery efficacy and homing.

Acknowledgments

This work was supported, in part, by National Institute of Biomedical Imaging and Bioengineering (R21 EB001785), National Cancer Institute (R21 CA102123, P50 CA114747, U54 CA119367, and R24 CA93862), Department of Defense (W81XWH-04-1-0697, W81XWH-06-1-0665, W81XWH-06-1-0042, and

DAMD17-03-1-0143), and a Benedict Cassen Postdoctoral Fellowship from the Education and Research Foundation of the Society of Nuclear Medicine (to WC). GN and ZX contributed equally to this work.

References

1. McConnell MJ, Imperiale MJ. Biology of adenovirus and its use as a vector for gene therapy. *Hum Gene Ther.* 2004; 15:1022–1033. [PubMed: 15610603]
2. Bergelson JM, Cunningham JA, Droguett G, et al. Isolation of a common receptor for Coxsackie B viruses and adenoviruses 2 and 5. *Science.* 1997; 275:1320–1323. [PubMed: 9036860]
3. Hemminki A, Kanerva A, Liu B, et al. Modulation of Coxsackie–adenovirus receptor expression for increased adenoviral transgene expression. *Cancer Res.* 2003; 63:847–853. [PubMed: 12591736]
4. Huard J, Lochmuller H, Acsadi G, et al. The route of administration is a major determinant of the transduction efficiency of rat tissues by adenoviral recombinants. *Gene Ther.* 1995; 2:107–115. [PubMed: 7719927]
5. Sullivan DE, Dash S, Du H, et al. Liver-directed gene transfer in non-human primates. *Hum Gene Ther.* 1997; 8:1195–1206. [PubMed: 9215737]
6. Tomanin R, Scarpa M. Why do we need new gene therapy viral vectors? Characteristics, limitations and future perspectives of viral vector transduction. *Curr Gene Ther.* 2004; 4:357–372. [PubMed: 15578987]
7. Akporiaye ET, Hersh E. Clinical aspects of intratumoral gene therapy. *Curr Opin Mol Ther.* 1999; 1:443–453. [PubMed: 11713758]
8. Mizuguchi H, Koizumi N, Hosono T, et al. A simplified system for constructing recombinant adenoviral vectors containing heterologous peptides in the HI loop of their fiber knob. *Gene Ther.* 2001; 8:730–735. [PubMed: 11406768]
9. Mizuguchi H, Hayakawa T. Adenovirus vectors containing chimeric type 5 and type 35 fiber proteins exhibit altered and expanded tropism and increase the size limit of foreign genes. *Gene.* 2002; 285:69–77. [PubMed: 12039033]
10. Mizuguchi H, Hayakawa T. Targeted adenovirus vectors. *Hum Gene Ther.* 2004; 15:1034–1044. [PubMed: 15610604]
11. Stevenson SC, Rollence M, Marshall-Neff J, McClelland A. Selective targeting of human cells by a chimeric adenovirus vector containing a modified fiber protein. *J Virol.* 1997; 71:4782–4790. [PubMed: 9151872]
12. Shayakhmetov DM, Papayannopoulou T, Stamatoyannopoulos G, Lieber A. Efficient gene transfer into human CD34(+) cells by a retargeted adenovirus vector. *J Virol.* 2000; 74:2567–2583. [PubMed: 10684271]
13. Koizumi N, Mizuguchi H, Utoguchi N, Watanabe Y, Hayakawa T. Generation of fiber-modified adenovirus vectors containing heterologous peptides in both the HI loop and C terminus of the fiber knob. *J Gene Med.* 2003; 5:267–276. [PubMed: 12692861]
14. Watkins SJ, Mesyanzhinov VV, Kurochkina LP, Hawkins RE. The ‘adenobody’ approach to viral targeting: specific and enhanced adenoviral gene delivery. *Gene Ther.* 1997; 4:1004–1012. [PubMed: 9415305]
15. Goldman CK, Rogers BE, Douglas JT, et al. Targeted gene delivery to Kaposi’s sarcoma cells via the fibroblast growth factor receptor. *Cancer Res.* 1997; 57:1447–1451. [PubMed: 9108444]
16. Sosnowski BA, Gu DL, D’Andrea M, Doukas J, Pierce GF. FGF2-targeted adenoviral vectors for systemic and local disease. *Curr Opin Mol Ther.* 1999; 1:573–579. [PubMed: 11249664]
17. Douglas JT, Miller CR, Kim M, et al. A system for the propagation of adenoviral vectors with genetically modified receptor specificities. *Nat Biotechnol.* 1999; 17:470–475. [PubMed: 10331807]
18. Fisher KD, Stallwood Y, Green NK, et al. Polymer-coated adenovirus permits efficient retargeting and evades neutralising antibodies. *Gene Ther.* 2001; 8:341–348. [PubMed: 11313809]
19. O’Riordan CR, Lachapelle A, Delgado C, et al. PEGylation of adenovirus with retention of infectivity and protection from neutralizing antibody *in vitro* and *in vivo*. *Hum Gene Ther.* 1999; 10:1349–1358. [PubMed: 10365665]

20. Croyle MA, Yu QC, Wilson JM. Development of a rapid method for the PEGylation of adenoviruses with enhanced transduction and improved stability under harsh storage conditions. *Hum Gene Ther.* 2000; 11:1713–1722. [PubMed: 10954905]
21. Croyle MA, Chirmule N, Zhang Y, Wilson JM. “Stealth” adenoviruses blunt cell-mediated and humoral immune responses against the virus and allow for significant gene expression upon readministration in the lung. *J Virol.* 2001; 75:4792–4801. [PubMed: 11312351]
22. Croyle MA, Chirmule N, Zhang Y, Wilson JM. PEGylation of E1-deleted adenovirus vectors allows significant gene expression on readministration to liver. *Hum Gene Ther.* 2002; 13:1887–1900. [PubMed: 12396620]
23. Eto Y, Gao JQ, Sekiguchi F, et al. PEGylated adenovirus vectors containing RGD peptides on the tip of PEG show high transduction efficiency and antibody evasion ability. *J Gene Med.* 2005; 7:604–612. [PubMed: 15543536]
24. Green NK, Herbert CW, Hale SJ, et al. Extended plasma circulation time and decreased toxicity of polymer-coated adenovirus. *Gene Ther.* 2004; 11:1256–1263. [PubMed: 15215884]
25. Lanciotti J, Song A, Doukas J, et al. Targeting adenoviral vectors using heterofunctional polyethylene glycol FGF2 conjugates. *Mol Ther.* 2003; 8:99–107. [PubMed: 12842433]
26. Ogawara K, Rots MG, Kok RJ, et al. A novel strategy to modify adenovirus tropism and enhance transgene delivery to activated vascular endothelial cells *in vitro* and *in vivo*. *Hum Gene Ther.* 2004; 15:433–443. [PubMed: 15144574]
27. Hynes RO. Integrins: bidirectional, allosteric signaling machines. *Cell.* 2002; 110:673–687. [PubMed: 12297042]
28. Guo W, Giancotti FG. Integrin signalling during tumour progression. *Nat Rev Mol Cell Biol.* 2004; 5:816–826. [PubMed: 15459662]
29. Jin H, Varner J. Integrins: roles in cancer development and as treatment targets. *Br J Cancer.* 2004; 90:561–565. [PubMed: 14760364]
30. Brooks PC, Montgomery AM, Rosenfeld M, et al. Integrin $\alpha_v\beta_3$ antagonists promote tumor regression by inducing apoptosis of angiogenic blood vessels. *Cell.* 1994; 79:1157–1164. [PubMed: 7528107]
31. Kerr JS, Slee AM, Mousa SA. The alpha v integrin antagonists as novel anticancer agents: an update. *Expert Opin Investig Drugs.* 2002; 11:1765–1774.
32. Shannon KE, Keene JL, Settle SL, et al. Anti-metastatic properties of RGD-peptidomimetic agents S137 and S247. *Clin Exp Metastasis.* 2004; 21:129–138. [PubMed: 15168730]
33. Burke PA, DeNardo SJ, Miers LA, et al. Cilengitide targeting of $\alpha_v\beta_3$ integrin receptor synergizes with radioimmunotherapy to increase efficacy and apoptosis in breast cancer xenografts. *Cancer Res.* 2002; 62:4263–4272. [PubMed: 12154028]
34. Gutheil JC, Campbell TN, Pierce PR, et al. Targeted antiangiogenic therapy for cancer using Vitaxin: a humanized monoclonal antibody to the integrin $\alpha_v\beta_3$. *Clin Cancer Res.* 2000; 6:3056–3061. [PubMed: 10955784]
35. Haubner R, Wester HJ, Weber WA, et al. Noninvasive imaging of $\alpha_v\beta_3$ integrin expression using ^{18}F -labeled RGD-containing glycopeptide and positron emission tomography. *Cancer Res.* 2001; 61:1781–1785. [PubMed: 11280722]
36. Chen X, Hou Y, Tohme M, et al. Pegylated Arg–Gly–Asp peptide: ^{64}Cu labeling and PET imaging of brain tumor $\alpha_v\beta_3$ -integrin expression. *J Nucl Med.* 2004; 45:1776–1783. [PubMed: 15471848]
37. Janssen ML, Oyen WJ, Dijkgraaf I, et al. Tumor targeting with radiolabeled $\alpha_v\beta_3$ integrin binding peptides in a nude mouse model. *Cancer Res.* 2002; 62:6146–6151. [PubMed: 12414640]
38. Chen X, Conti PS, Moats RA. *In vivo* near-infrared fluorescence imaging of integrin $\alpha_v\beta_3$ in brain tumor xenografts. *Cancer Res.* 2004; 64:8009–8014. [PubMed: 15520209]
39. Liang Q, Nguyen K, Satyamurthy N, et al. Monitoring adenoviral DNA delivery, using a mutant herpes simplex virus type 1 thymidine kinase gene as a PET reporter gene. *Gene Ther.* 2002; 9:1659–1666. [PubMed: 12457279]
40. Xiong Z, Cheng Z, Zhang X, et al. Imaging chemically modified adenovirus for targeting tumors expressing integrin $\alpha_v\beta_3$ in living mice with mutant herpes simplex virus type 1 thymidine kinase PET reporter gene. *J Nucl Med.* 2006; 47:130–139. [PubMed: 16391197]

41. Read ML, Etrych T, Ulbrich K, Seymour LW. Characterisation of the binding interaction between poly(L-lysine) and DNA using the fluorescamine assay in the preparation of non-viral gene delivery vectors. *FEBS Lett.* 1999; 461:96–100. [PubMed: 10561503]
42. Smith AE. Viral vectors in gene therapy. *Annu Rev Microbiol.* 1995; 49:807–838. [PubMed: 8561480]
43. Thomas CE, Ehrhardt A, Kay MA. Progress and problems with the use of viral vectors for gene therapy. *Nat Rev Genet.* 2003; 4:346–358. [PubMed: 12728277]
44. Wu JC, Sundaresan G, Iyer M, Gambhir SS. Noninvasive optical imaging of firefly luciferase reporter gene expression in skeletal muscles of living mice. *Mol Ther.* 2001; 4:297–306. [PubMed: 11592831]
45. Zhang X, Xiong Z, Wu X, et al. Quantitative PET imaging of tumor integrin $\alpha v\beta 3$ expression with [^{18}F]FRGD2. *J Nucl Med.* 2005; 47:492–501. [PubMed: 16513619]
46. Alemany R, Suzuki K, Curiel DT. Blood clearance rates of adenovirus type 5 in mice. *J Gen Virol.* 2000; 81:2605–2609. [PubMed: 11038370]
47. Mok H, Palmer DJ, Ng P, Barry MA. Evaluation of polyethylene glycol modification of first-generation and helper-dependent adenoviral vectors to reduce innate immune responses. *Mol Ther.* 2005; 11:66–79. [PubMed: 15585407]
48. Rolland A, Collet B, Le Verge R, Toujas L. Blood clearance and organ distribution of intravenously administered polymethacrylic nanoparticles in mice. *J Pharm Sci.* 1989; 78:481–484. [PubMed: 2760823]
49. Doran JE, Lundsgaard-Hansen P. Role of the reticuloendothelial system in the pathogenesis of organ damage. *Br J Hosp Med.* 1988; 39:221–225. [PubMed: 3282588]
50. Contag CH, Bachmann MH. Advances in *in vivo* bioluminescence imaging of gene expression. *Annu Rev Biomed Eng.* 2002; 4:235–260. [PubMed: 12117758]
51. Gross S, Piwnica-Worms D. Spying on cancer: molecular imaging *in vivo* with genetically encoded reporters. *Cancer Cell.* 2005; 7:5–15. [PubMed: 15652745]
52. Gambhir SS, Barrio JR, Phelps ME, et al. Imaging adenoviral-directed reporter gene expression in living animals with positron emission tomography. *Proc Natl Acad Sci USA.* 1999; 96:2333–2338. [PubMed: 10051642]
53. Gambhir SS, Bauer E, Black ME, et al. A mutant herpes simplex virus type 1 thymidine kinase reporter gene shows improved sensitivity for imaging reporter gene expression with positron emission tomography. *Proc Natl Acad Sci USA.* 2000; 97:2785–2790. [PubMed: 10716999]

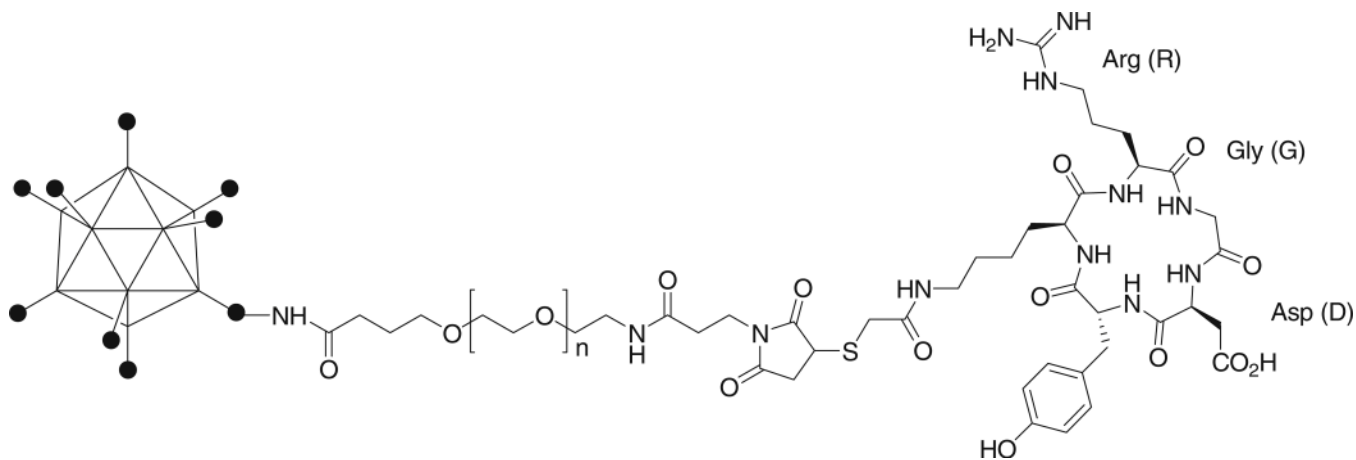


Fig. 1. RGD-PEG-AdLuc conjugate. The adenoviral (Ad) vector encoding firefly luciferase (AdLuc) was connected with cyclic RGD peptide through a bifunctional poly(ethylene glycol) (PEG; MW = 3,400) linker. The *N*-hydroxysuccinimide ester on one end of the PEG reacts with primary amino groups on the AdLuc surface and the other end of the PEG reacts with the thiolated RGD peptide.

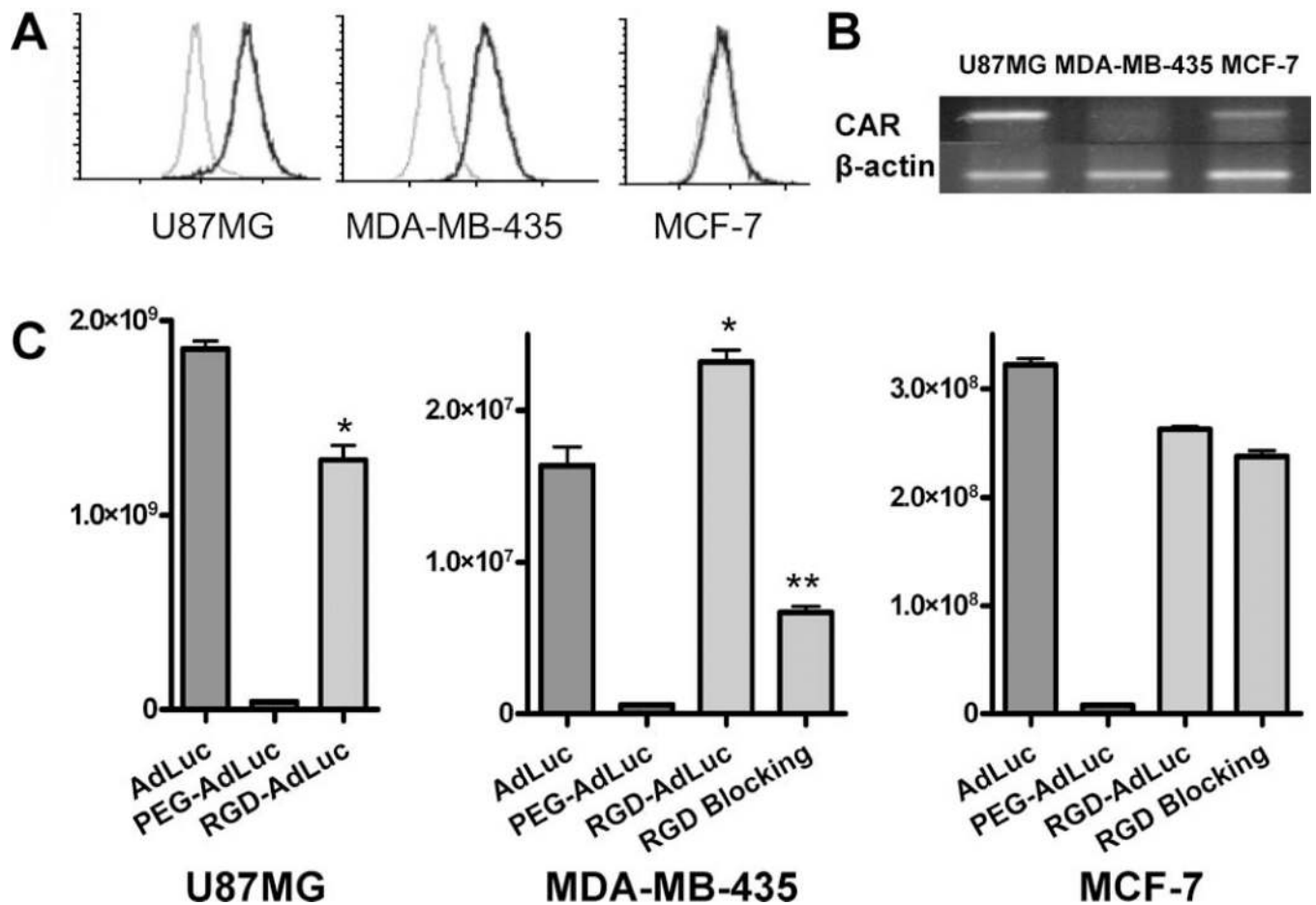


Fig. 2.

Transduction of AdLuc, PEG-AdLuc, and RGD-PEG-AdLuc in U87MG, MDA-MB-435, and MCF-7 cells. **(A)** The expression of integrin $\alpha_v\beta_3$ was determined by flow cytometry. **(B)** mRNA level of CAR was determined by reverse transcriptase PCR. **(C)** Luciferase activity was measured in U87MG, MDA-MB-435, and MCF-7 cells upon transduction with adenoviral vectors. RGD blocking was performed in the presence of 20 $\mu\text{g/ml}$ of free RGD. Luciferase activity is normalized and expressed as photon per second per million cells. Data were measured as the mean of triplicates \pm SD. * $P < 0.05$, ** $P < 0.01$

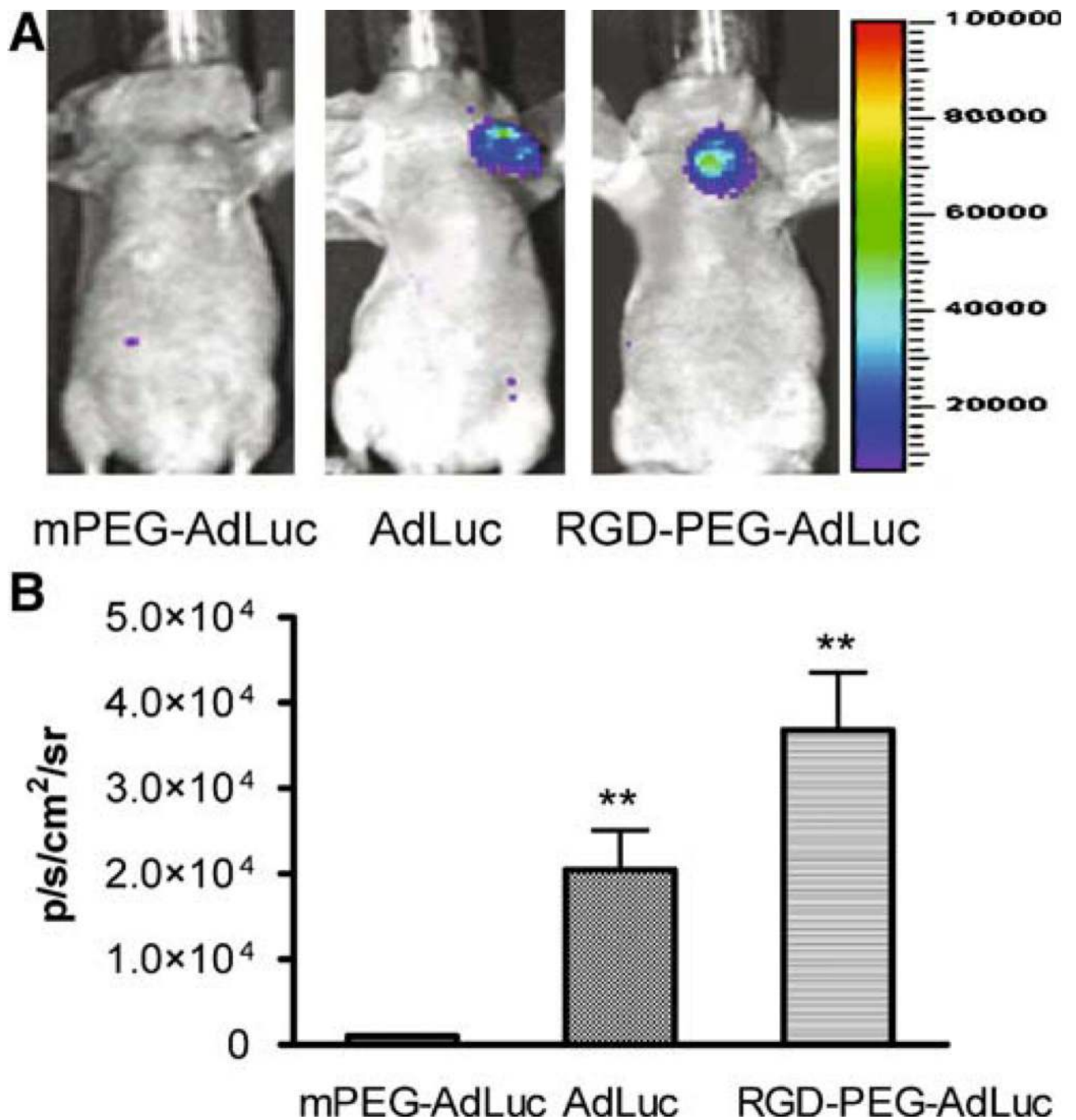


Fig. 3. Bioluminescence imaging of intratumorally injected vectors. Orthotopic MDA-MB-435 breast cancer tumor-bearing female nude mice ($n = 3$ per group) were injected intratumorally with AdLuc, PEG-AdLuc, or RGD-PEG-AdLuc (2.5×10^9 vp/kg) and then imaged using the Xenogen IVIS200 system at 48 hours after virus administration. **(A)** Ventral luciferase signal from the tumor at ten minutes after intraperitoneal injection of D-luciferin substrate (10 mg/kg). **(B)** Photon flux recorded from ROI analysis of the MDA-MB-435 tumor is normalized as average radiance ($\text{p s}^{-1} \text{cm}^{-2} \text{sr}^{-1}$). * $P < 0.05$, ** $P < 0.01$

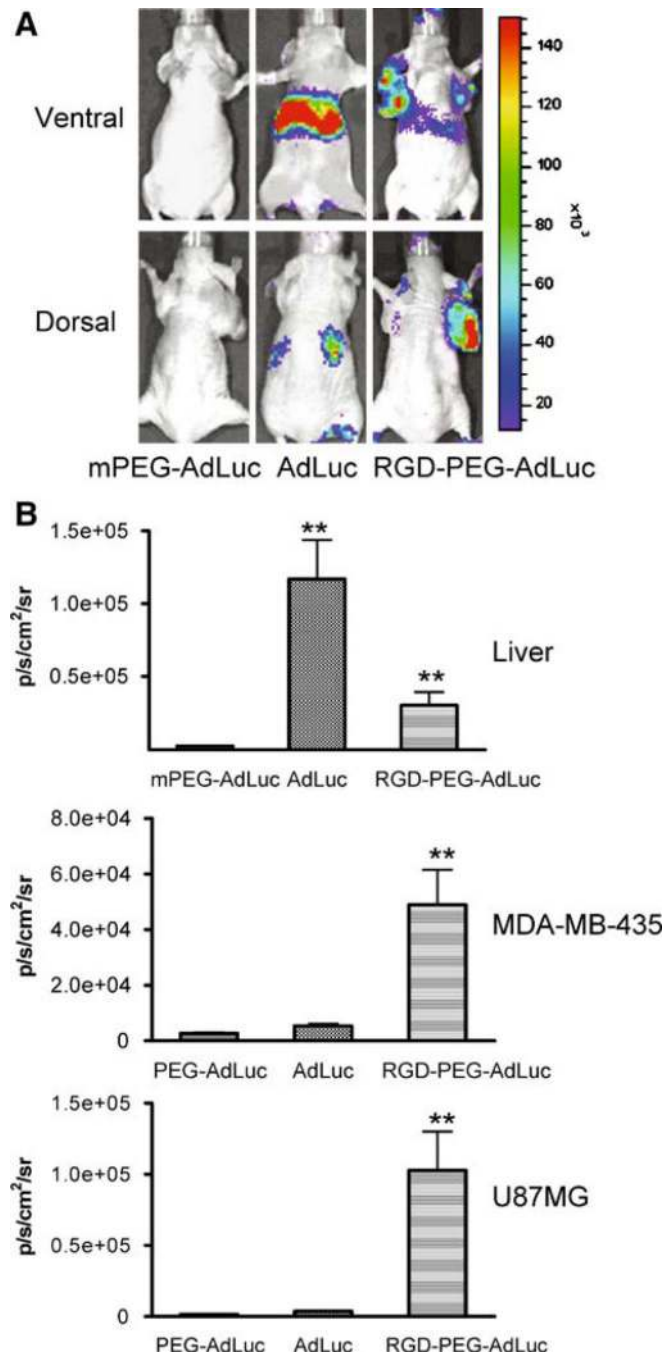


Fig. 4. Bioluminescence imaging of intravenously injected vectors. Female athymic nude mice bearing both subcutaneous U87MG glioma and orthotopic MDA-MB-435 breast cancer tumors ($n = 3/\text{group}$) were intravenously injected with AdLuc, PEG-AdLuc, or RGD-PEG-AdLuc (1.25×10^{12} vp/kg) and then imaged using the Xenogen IVIS200 system at 48 hours after virus administration. The U87MG tumor inoculated on the right front arm is best visualized at the prone position. The MDA-MB-435 tumor and liver signals are best visualized at the supine position. **(A)** Dorsal and ventral luciferase signals from

representative tumor mice imaged at ten minutes after intraperitoneal injection of ^{125}I -luciferin substrate (10 mg/kg). **(B)** Photon flux recorded from ROI analysis of the liver (ventral), MDA-MB-435 tumor (ventral) and U87MG tumor (dorsal) normalized as average radiance ($\text{p s}^{-1} \text{ cm}^{-2} \text{ sr}^{-1}$). * $P < 0.05$, ** $P < 0.01$

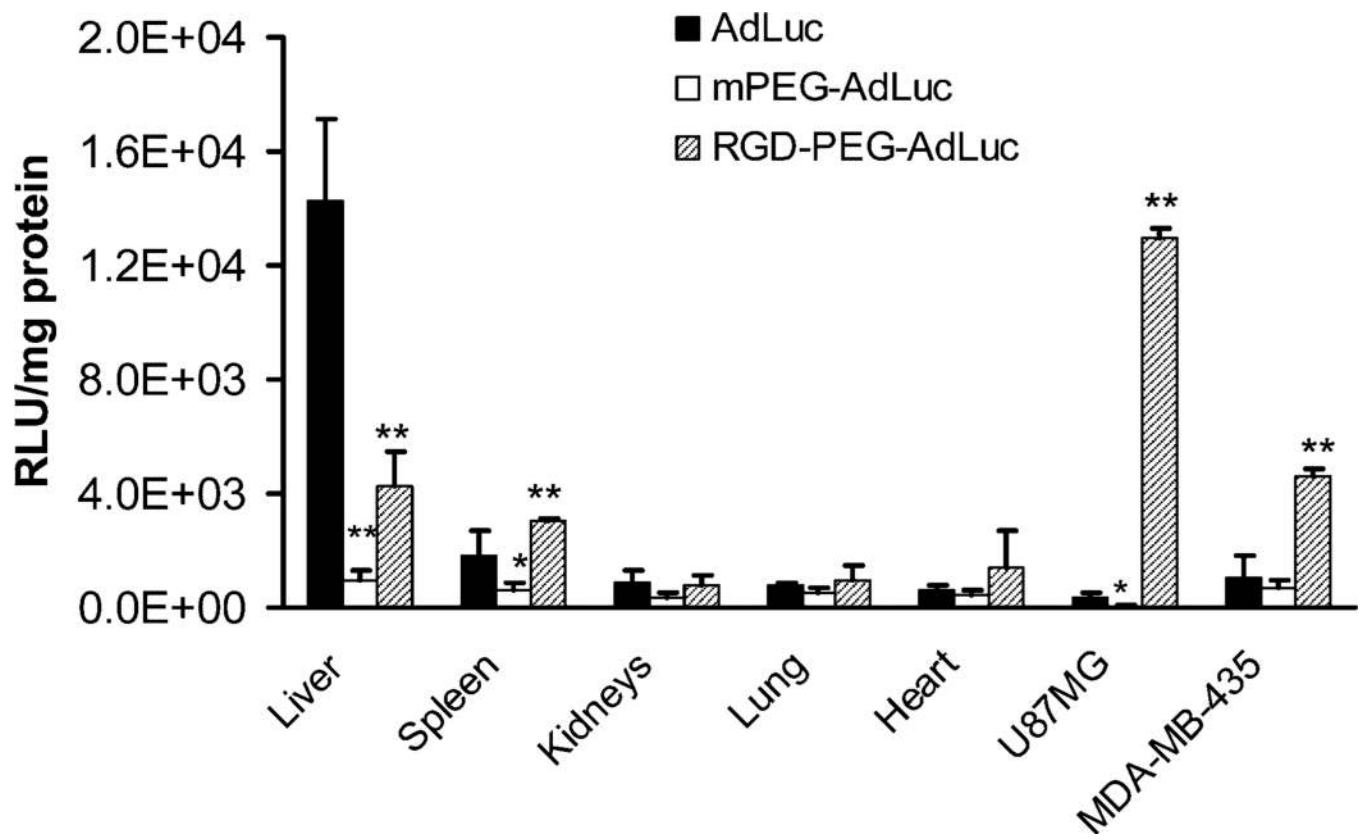


Fig. 5. Luciferase activity in the tumors and major organs from tumor-bearing mice at 24 hours after noninvasive bioluminescence imaging. Results were expressed as the mean RLU \pm SD. * $P < 0.05$, ** $P < 0.01$ compared to AdLuc